Electrodeposition of Nickel Hydroxide Films on Nickel Foil and Its Electrochemical Performances for Supercapacitor

Guo-rui Fu, Zhong-ai Hu[*]*, Li-jing Xie, Xiao-qing Jin, Yu-long Xie,Yao-xian Wang, Zi-yu Zhang, Yu-ying Yang, Hong-ying Wu*

Key Laboratory of Polymer Material of Gansu Province, College of Chemistry and Chemical Engineering, Northwest Normal University, Lanzhou 730070, Gansu, P. R. China
[*]E-mail: zhongai@nwnu.edu.cn

Nickel hydroxide was prepared by electrodeposition in $Ni(NO_3)_2$ aqueous solution for the electrode materials of supercapacitors. The structure and morphology of products were characterized using X-ray diffraction (XRD) and field emission scanning electron microscopy (FESEM), respectively. The experimental results of XRD show that the products are typical α-phase nickel hydroxide. The FESEM results reveal that the α-$Ni(OH)_2$ displays particle-like morphology with a loosely packed structure. The component and thermal stability of the products are respectively measured by FT-IR, thermogravimetry and differential thermal analysis (TG/DTA). The electrochemical performances are investigated by cyclic voltammetry (CV) and galvanostatic charge-discharge technique in 1 M KOH electrolyte. The results show that the α-$Ni(OH)_2$ with particle-like morphology has excellent electrochemical performances and its specific capacitance value as single electrode is up to 2595 F g^{-1}. Furthermore, the effect of deposition conditions such as deposition potential and concentration of $Ni(NO_3)_2$ solution on the electrochemical capacitance of the deposited $Ni(OH)_2$ films is discussed in detail.

1. INTRODUCTION

Electrochemical capacitors (ECs), also called supercapacitors or ultracapacitors, have raised considerable attention over the past decades because of their higher power density and longer cycle life than secondary batteries and their higher energy density compared to conventional electrical double-layer capacitors [1–4]. They have many practical applications such as auxiliary power sources in combination with fuel cells or batteries for hybrid electric vehicles, back up and pulse power sources for mobile electric devices, etc [5].

Base upon their charge-storage mechanisms, supercapacitors can be classified into two types. One is the electric double-layer capacitor, and the other is the redox capacitor. In the former, energy storage arises mainly from the separation of electronic and ionic charges at the interface between electrode materials with high-specific area (such as carbon) and the electrolyte solution. In the latter, fast Faradaic reactions take place at the electrode materials at characteristic potentials, as in batteries [6]. To develop an advanced ECs device, an active electrode material with high capacity performance is indispensable [7]. Initially, noble metal oxides exhibit much higher specific capacitance than conventional carbon materials and better electrochemical stability than electronically conducting polymer materials, such as RuO_2 [8–11] have exhibited prominent properties among various pseudocapacitor materials. Hu and Chen [11] reported that the specific capacitance of RuO_2 was even as high as 1500 F g^{-1} in RuO_2/AC composite electrode. However, the high cost of these noble metal materials limits it from commercialization. Therefore, the development of alternative inexpensive electrode materials with high performance has been one of the most active research fields of electrochemistry during the last few years. Several transition metal oxides and hydroxides have been investigated e.g. NiO [12], CoOx [13], MnO_2 [14], $Ni(OH)_2$ [15], $Co(OH)_2$ [16], etc. Among these candidates, $Ni(OH)_2$ is known as a promising electrode material for applications in energy/power storage devices, especially ECs, is attractive in view of its low cost, its well-defined electrochemical redox activity and the possibility of enhanced performance through different preparative method [17-21]. However, only few papers are reported for the capacitive behavior of the $Ni(OH)_2$ up to now [22, 23]. Accordingly, more and further studies on the capacitive properties of the $Ni(OH)_2$ are needed. Among the existing synthetic approaches to the $Ni(OH)_2$ materials [22, 23], electrochemical techniques are of great interest due to their unique principles and flexibility in the control of the structure and morphology of the film materials [24, 25]. The main advantage of the electrodeposition technique is its relatively easy and accurate control of the surface microstructure of deposited films by changing deposition variables, such as electrolyte, deposition potential, bathing temperature, and so forth [21]. Such as, Yiwei Tan et al. electrochemical deposited mesoporous $Ni(OH)_2$ films from dilute surfactant solutions [26]. Vinay Gupta et al. synthesized $Co(OH)_2$ by the potentiostatic deposition route [27].

In this work, we report the electrochemical synthesis of α-$Ni(OH)_2$ films which are directly electrodeposited on nickel foil in $Ni(NO_3)_2 \cdot 6H_2O$ aqueous solution. The effect of deposition conditions such as deposition potential and concentration of $Ni(NO_3)_2$ solution on the electrochemical capacitance of the deposited $Ni(OH)_2$ films is discussed in detail. A maximum specific capacitance value of 2595 F g^{-1} is obtained for the $Ni(OH)_2$ films deposited at -0.90 V versus Ag/AgCl electrode, which indicate it is a promising supercapacitor electrode material.

2. EXPERIMENTAL PART

2.1. Synthesis of Ni(OH)₂

Reagents were all of AR grade. Water used in the synthesis and washing was deionized. Research grade nickel foil was purchased from Shanghai metal foil plant. The nickel foil was polished

with emery paper to a rough finish, washed in an ultrasonic bath of acetone, dilute NaOH and dilute HNO_3 in turn for 10 min, rinsed with deionized water and then air-dried prior to use. The nanostructured nickel hydroxide films were deposited from 0.08 M $Ni(NO_3)_2 \cdot 6H_2O$ aqueous solution at a potential of -0.90 V vs. Ag/AgCl (saturated KCl solution) electrode. The electrodeposition was conducted using a Chenhua CHI660B model Electrochemical Workstation (Shanghai), with a three-electrode cell consisting of nickel foil working electrode (1 cm^2 in area), a platinum foil counter electrode and a Ag/AgCl (saturated KCl solution) reference electrode. The deposited electrode was washed with deionized water several times, then left to dry at room temperature in prior to characterize. All electrodepositions of nickel hydroxide films were performed under both potentiostatic and room temperature.

2.2. Materials characterization

The structure of the nickel hydroxide was examined by X-ray diffraction (XRD) (D/Max-2400) with Cu Kα radiation (λ=1.5418 Å) operating at 40 kV, 60 mA. The components of materials were measured by a Nicolet Nexus 670 FT–IR instrument. The morphology and size of nanoparticles was observed by FESEM (JSM–6701F, Japan). Thermal analyses, including thermogravimetry and differential thermal analysis were carried out using a Perkin-Elmer TG/DTA–6300 instrument in the temperature range of 25–750 °C. A heating rate of 10 °C min^{-1} in nitrogen with a flow rate of 20 mL min^{-1} was used.

2.3. Electrochemical characterization

The freshly prepared $Ni(OH)_2$ films on nickel foil substrate was directly used as the working electrode. A typical three-electrode experimental cell equipped with a working electrode, a platinum foil counter electrode, and a Ag/AgCl reference electrode was used for measuring the electrochemical properties of working electrode and its performance as a faradaic supercapacitor. All electrochemical measurements were carried out in 1 mol/L KOH aqueous solution as electrolyte. Cyclic voltammetry (CV) and galvanostatic charge-discharge were carried out on a CHI660B electrochemical working station (CH Instrument) at room temperature.

All solutions used in this work were prepared with double-distilled water. All electrochemical experiments were carried out at room temperature and the potentials were referred to Ag/AgCl (saturated KCl solution) electrode.

3. RESULTS AND DISCUSSION

It is demonstrated that the electrodeposition process of the $Ni(OH)_2$ films could include an electrochemical reaction and a precipitation reaction expressed as follows [28]:

$$NO^-_3 + 7H_2O + 8e^- \rightarrow NH^+_4 + 10OH^- \quad (1)$$
$$Ni^{2+} + 2OH^- \rightarrow Ni(OH)_2 \quad (2)$$
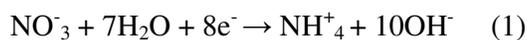
When electric current passes the electrolyte containing $Ni(NO_3)_2$, nitrate ions can be reduced on the cathodic surface to produce hydroxide ions. The generation of OH^- at the cathode raises the local pH, resulting in the precipitation of $Ni(OH)_2$ at the electrode surface.

3.1. XRD analysis of Ni(OH)₂

The crystal phase and structure information on the products were obtained by XRD measurements. Fig. 1 shows XRD patterns of the products peeled from nickel foil substate. All the diffraction peaks can be indexed to the diffraction data of the $Ni(OH)_2·0.75H_2O$ (JCPDS, No. 38-0715). This is a typical α-type $Ni(OH)_2$. Except the diffraction peak indexed as (110), the others are broad, with a sharp rise in intensity followed by a pronounced asymmetry on the higher angle side. These ''saw-tooth'' reflections are typical of turbostratic phases which are ordered in two dimensions, but whose layers are orientationally disordered. In general, the broadening of XRD diffraction peaks may result from small grain sizes or structural microdistortions in crystal. Under the present experimental conditions, the extremely small particle-like structure results in a significant broadening of some diffraction peaks in $Ni(OH)_2$ XRD patterns. This can be confirmed by FESEM images.
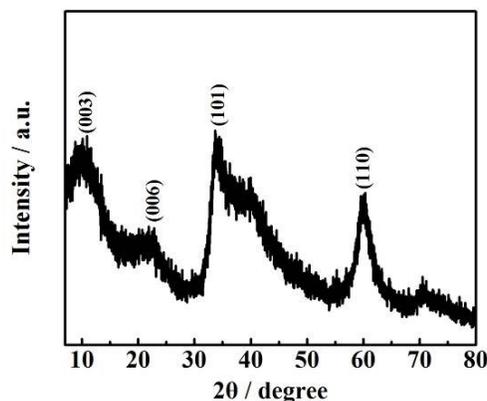
**Figure 1.** XRD patterns of the $Ni(OH)_2$

3.2. FT-IR analysis of Ni(OH)₂

To further support the XRD study, the FT-IR spectrum of the samples was presented in Fig. 2. The spectrum shows a typical features of α-$Ni(OH)_2$. The broad and intense band centered at 3448 cm^{-1} is assigned to the O–H stretching vibration of interlayer water molecules and of H-bound OH group. But the sharp peak attributed to O-H stretching mode of the free Ni-OH groups disappears due to the existence of hydrogen bonding between the hydrogen atoms and the intercalated anions or water molecules within the layers. The peak at 1632 cm^{-1} is due to the bending vibration of water molecules. The weak peaks around 1475 cm^{-1} and 1051 cm^{-1} are assigned to carbonate ions and their existence could be attributed to the dissolution of CO_2 from air. The other absorption bands are relative to

carbonate ions was too weak to be identifiable, implying a low content of carbonate ions. The intense and sharp band at 1383 cm^{-1} is characteristic of interlayer NO_3^-. The band at about 648 cm^{-1} is attributed to the δNi–O–H vibration. A small weak peak centered around 467 cm^{-1} is assigned to the Ni–O stretching vibration [29–31].
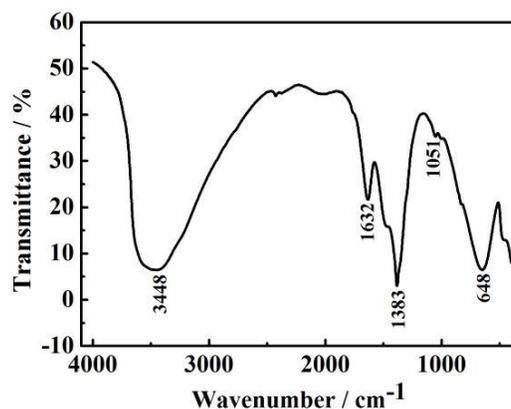
Figure 2. FT-IR spectra of the Ni(OH)$_2$

3.3. FESEM analysis of Ni(OH)$_2$

The surface morphology of the Ni(OH)$_2$ films was investigated by FESEM and the micrographs were shown in Fig. 3. In the low magnification, the as-prepared samples seem to be uniform particles. However, in the high magnification these particles are not solid, but consist of several uniform nano-particles. It possesses loosely packed structure, and it is advantageous for the electrolyte ions to access the active materials and result in Faraday reaction, and the H$^+$ or OH$^-$ yielded to migrate in time, which may contribute to enhancement of capacitive performance.
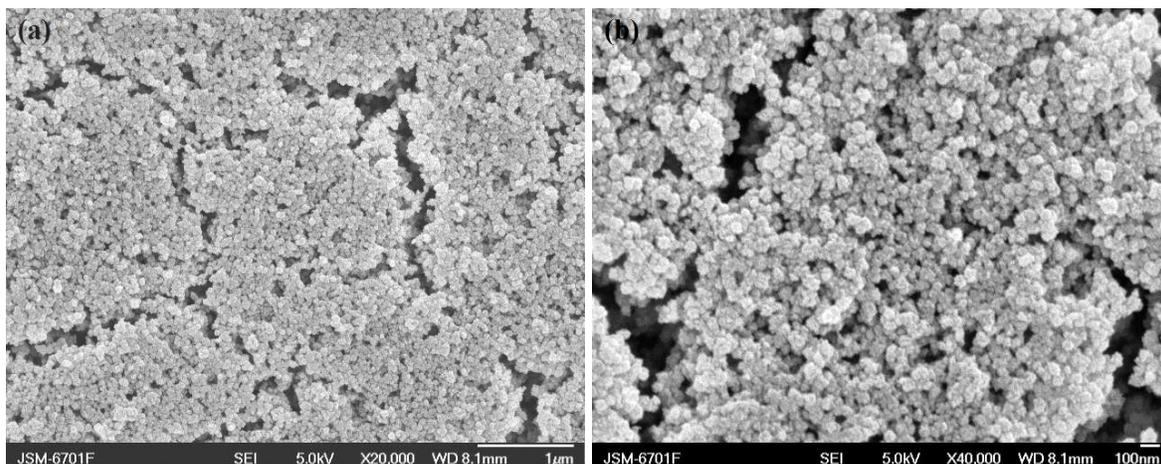
Figure 3. FESEM images of the Ni(OH)$_2$: (a) low magnification (b) high magnification

3.4. TG–DTA analysis of Ni(OH)₂

Fig. 4 depicts the typical TG–DTA curves of the samples. There are two endothermic peaks at 87.3 °C and 264.7 °C on the DTA curve. Correspondingly, the TG curve has two sharp weight losses with 13.7 wt% and 20.3 wt%. The former corresponds to the evaporation of the adsorbed and intercalated water molecules between 25 °C and 187.5 °C, the latter is associated with the loss of water produced by dehydroxylation of the hydroxide layers combined with the partial loss of the anionic species (CO_3^{2-} and NO_3^-) between 187.5 °C and 400 °C.
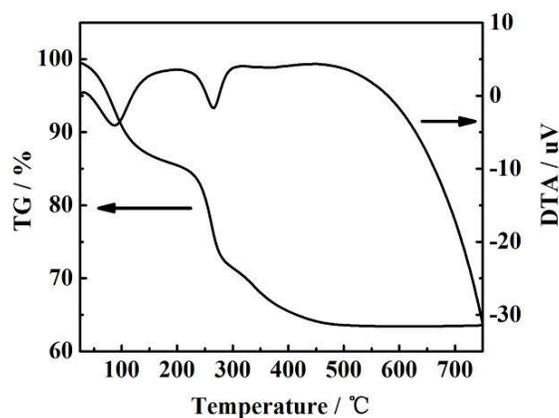

Figure 4. TG/DTA curves of the Ni(OH)₂

3.5. Electrochemical behavior of Ni(OH)₂ films electrode

Cyclic voltammetry (CV) is considered to be a suitable tool to indicate the capacitive behavior of any material. Fig. 5 presents the CV curves of the samples in 1 M KOH electrolyte at the scan rates of 5, 10, 15, 20 and 30 mV s⁻¹. As shown in Fig. 5, there is a pair of strong redox peaks as a result of the Faradaic reactions of the Ni(OH)₂. For the Ni(OH)₂ electrode material, it is well known that the surface faradic reactions will proceed according to the following reaction [32].

$$Ni(OH)_2 + OH^- = NiOOH + H_2O + e^- \qquad (3)$$

The anodic peak is due to the oxidation of Ni(OH)₂ to NiOOH, and the cathodic peak is for the reverse process. One quasi-reversible electron transfer process is visible in the CV curve, indicating that the measured capacitance is mainly based on redox mechanism [33]. Moreover, the shape of curves (Fig.5) displayed that the capacitance characteristic was distinct from that of the electric double layer capacitor, which would produce a CV curve is usually close to an ideal rectangular shape. Because solution and electrode resistance can distort current response at the switching potential and this distortion is dependent upon the scan rate [34], as can be seen from Fig. 5, the shape of CV curves of

the Ni(OH)$_2$ films are not significantly influenced with the increasing of the scan rates. This indicated that the improved mass transportation and electron conduction within the material. Furthermore, the insert of Fig. 5 reveals that the anodic peak current i_p vs. $V^{1/2}$ plot, where V is the voltage scan rate, gives a reasonable linear relationship. It can be indicated that the redox reactions of nickel hydroxide is a diffusion-limited reaction.
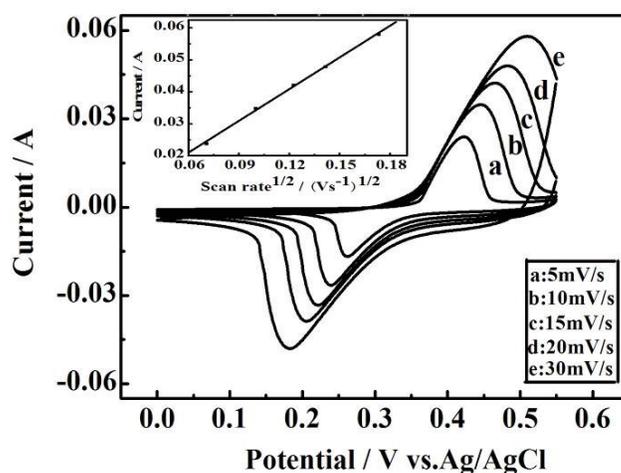

Figure 5. Cyclic voltammograms of the Ni(OH)$_2$ at different scan rates. Variation of anodic peak current with scan rate$^{1/2}$ for the Ni(OH)$_2$ (insert)

Electrochemical capacitance behavior of the Ni(OH)$_2$ films electrode was investigated by chronopotentiometry in 1 M KOH aqueous solution. Fig. 6a shows the charge–discharge curves of the Ni(OH)$_2$ films electrode measured at different current densities within the potential window of 0 to 0.45 V. The shape of the charge–discharge curves does not present the characteristic of a pure electric double layer capacitor, but mainly pseudocapacitance, which corresponds with the result of the CV test. The specific capacitance is calculated by $I \times \Delta t/(\Delta V \times m)$, where I is the constant discharging current, Δt is the discharging time, ΔV is the potential drop during discharge, and m is the mass of the Ni(OH)$_2$ [13], the mass of active material is estimated by Faraday's law on the assumption that faraday current efficiency for deposition is 100% [21]. The specific capacitance values are calculated to be 2595, 2320, 2004, 1900.8 and 1784 F g^{-1} corresponding to the dischargeing current densities of 1, 2, 5, 7, and 10 A g^{-1}, respectively. Fig. 6b shows the charge–discharge curves of the Ni(OH)$_2$ films electrode measured at a current density of 10 A g^{-1}. The variation of the specific capacitance with the current density is shown in Fig. 6c. This Ni(OH)$_2$ films electrode possesses excellent capacitance at all the current densities and the relatively small capacitance decrease is caused by the large voltage (IR) drop and the insufficient active material involved in the redox reaction under higher current densities. These results suggest the Ni(OH)$_2$ films electrode has a good rate capability at a large current density, which is very important for the electrode materials of a supercapacitor to provide high power density.
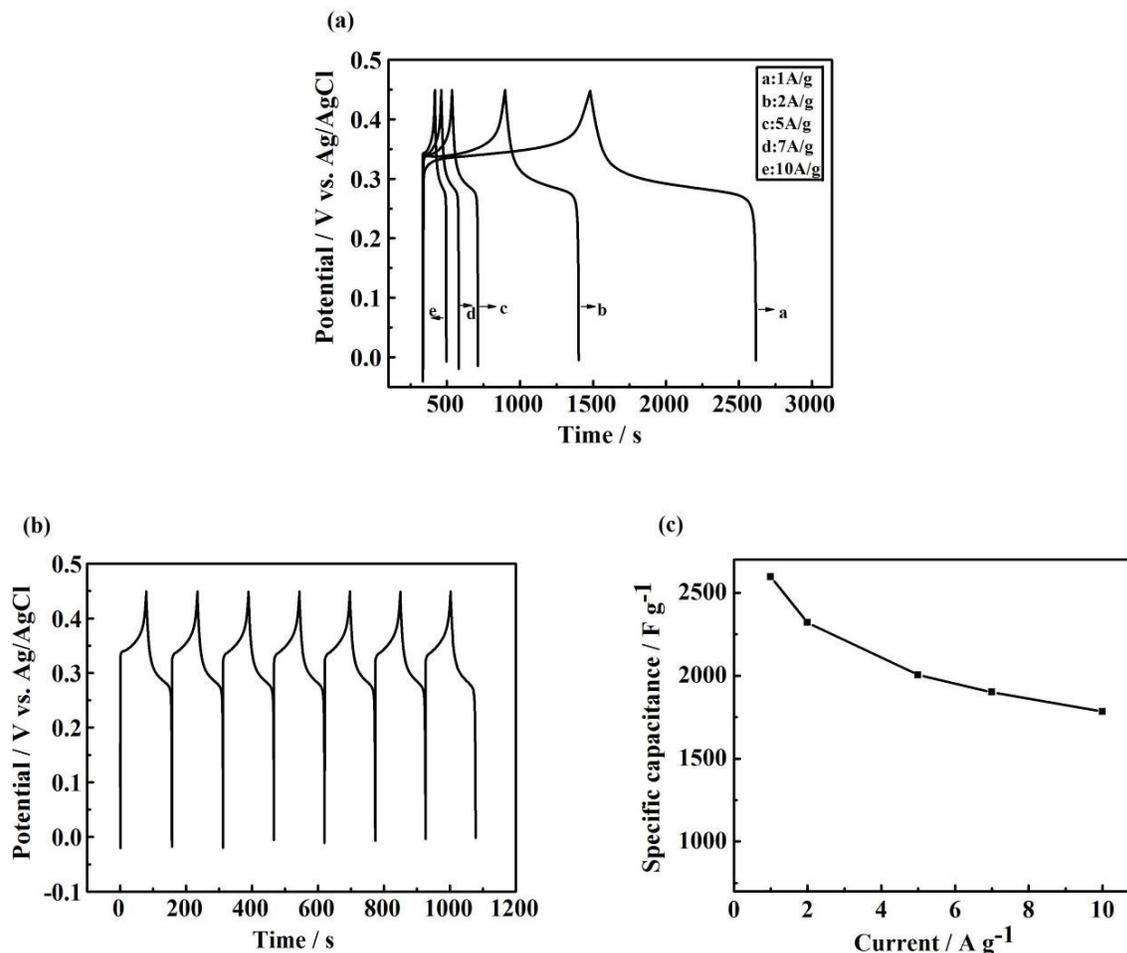
Figure 6. (a) Charge–discharge behavior of the $Ni(OH)_2$ films electrode at different current densities, (b) at current density of 10 A g^{-1}, (c) Dependence of specific capacitance on the current density for nickel hydroxide

The effect of the deposition conditions on the electrochemical capacitance of the deposited $Ni(OH)_2$ films is discussed in detail. Fig. 7 and Fig. 8 present that the effect of the concentration of $Ni(NO_3)_2$ and the potential of electrodeposition on the specific capacitance, respectively. As shown in Fig. 7, the maximum specific capacitance value was obtained when the concentration of $Ni(NO_3)_2$ solution was 0.08 M. So the concentration of $Ni(NO_3)_2$ solution lower or higher than 0.08 M is unfavorable to obtain the higher specific capacitance value. Likewise, the maximum specific capacitance value was obtained at a potential of -0.90 V vs. Ag/AgCl electrode and other deposition conditions are not changed, as shown in Fig. 8. The high $Ni(NO_3)_2$ concentration and high current density can perhaps speed the nucleation and growth of α-$Ni(OH)_2$, which maybe result in the morphology, size of particles or structure of α-$Ni(OH)_2$ that is disadvantageous for enhancement of α-$Ni(OH)_2$ capacitance. Furthermore, the α-$Ni(OH)_2$ shows very stable specific capacitance values for different deposited mass, as shown in Fig. 9.
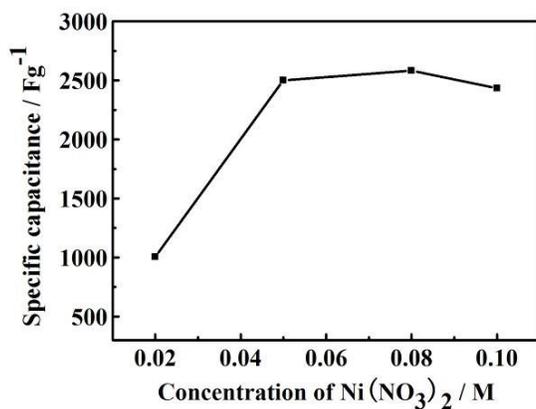
Figure 7. Dependence of specific capacitance on the concentration of Ni(NO$_3$)$_2$
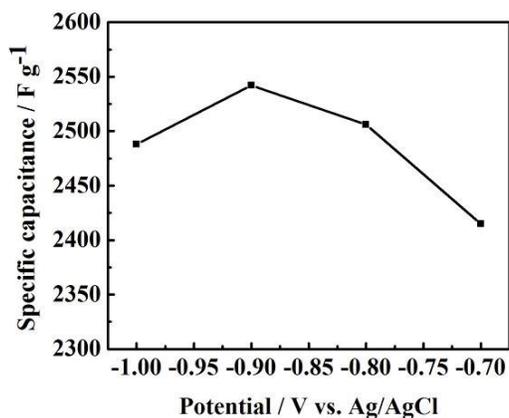
Figure 8. Dependence of specific capacitance on the potential of electrodeposition
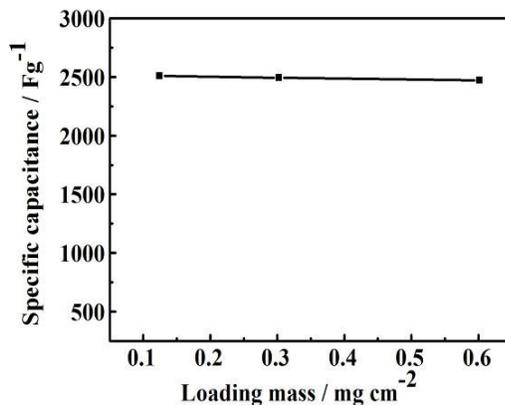
Figure 9. Dependence of specific capacitance on the loading mass for Ni(OH)$_2$

4. CONCLUSIONS

Particle-like nickel hydroxide for electrochemical capacitors has been successfully synthesized by electrodeposition technique on nickel foil. The XRD results confirm that the synthesized samples are pure α-Ni(OH)$_2$. The unique microstructure is responsible for the good electrochemical capacitance performance, which creates the fast electrochemical accessibility of the electrolyte and OH$^-$ ions to the bulk of the Ni(OH)$_2$ phase, providing an important morphological basis for a high specific capacitance. The maximum specific capacitance of 2595 F g^{-1} was obtained for the α-Ni(OH)$_2$ at a constant current charge/discharge test of 1 A g^{-1}. The α-Ni(OH)$_2$ also reveals the stable reversible characteristics at high current density. It implies that the α-Ni(OH)$_2$ synthesized here can be of significant importance for practical application. The results indicate that the optimal deposition conditions is deposition potential of -0.90 V (vs. Ag/AgCl) and the Ni(NO$_3$)$_2$ aqueous solution of 0.08 M.

References

1. B. E. Conway, Electrochemical Supercapacitors, Scientific Fundamentals and Technological Applications, Kluwer Academic/Plenum Press, New York (1999)
2. M. Winter, R. J. Brodd, *Chem. Rev.*, 104 (2004) 4245
3. H. Y. Lee, J. B. Goodenough, *J. Solid State Chem.*, 144 (1999) 220
4. D. Liu, Q. Zhang, P. Xiao, B. B. Garcia, Q. Guo, R. Champion, G. Cao, *Chem. Mater.*, 20 (2008) 1376
5. R. A. Huggins, *Solid State Ionics.*, 134 (2000) 179
6. J. H. Park, J. M. Ko, O. O. Park, D. W. Kim, *J. Power Sources.*, 105 (2002) 20
7. C. C. Hu, K. H. Chang, M. C. Lin, Y. T. Wu, *Nano Lett.*, 12 (2006) 2690
8. J. P. Zheng, P. J. Cygan, T. R. Zow, *J. Electrochem. Soc.*, 142 (1995) 2699
9. G. Arabale, D. Wagh, M. Kulkarni, I. S. Mulla, S. P. Vernkar, K. Vijamohanan, A. M. Rao, *Chem. Phys. Lett*., 376 (2003) 207
10. Y. G. Wang, X. G. Zhang, *Electrochem. Acta.*, 49 (2004) 1957
11. C. C. Hu, W. C. Chen, *Electrochem. Acta.*, 49 (2004) 3469
12. W. Xing, F. Li, Z. F. Yan, G. Q. Lu, *J. Power Sources.*, 134 (2004) 324
13. C. Lin, J. A. Ritter, B. N. Popov, *J. Electrochem. Soc*., 145 (1998) 4097
14. S. C. Pang, M. A. Anderson, T. W. Chapman, *J. Electrochem. Soc.*, 147 (2000) 444
15. L. Cao, L. B. Kong, Y. Y. Liang, H. L. Li, *Chem. Commun*., 14 (2004) 1646
16. L. Cao, F. Xu, Y. Y. Liang, H. L. Li, *Adv. Mater.*, 16 (2004) 1853
17. H. Bode, K. Dehmelt, J. Witte, *Electrochim. Acta.*, 11 (1966) 1079
18. T. N. Ramesh, R. S. Jayashree, P. V. Kamath, S. Rodrigues, A. K. Shukla, *J. Power Sources.*, 104 (2002) 295
19. W. K. Hu, D. Noreus, *Chem. Mater.*, 15 (2003) 974
20. Z. Chang, H. Tang, J. G. Chen, *Electrochem. Commun.*, 1 (1999) 513
21. D. D. Zhao, W. J. Zhou, H. L. Li, *Chem. Mater.*, 19 (2007) 3882
22. M. S. Wu, H. H. Hsieh, *Electrochimica Acta.*, 53 (2008) 3427

23. Q. H. Huang, X. Y. Wang, J. Li, C. L. Dai, S. Gamboa, P. J. Sebastian, *Journal of Power Sources.*, 164 (2007) 425
24. G. S. Attard, P. N. Bartlett, N. R. B. Coleman, J. M. Elliott, J. R. Owen, J. H. Wang, *Science.*, 278 (1997) 838
25. P. A. Nelson, J. M. Elliott, G. S. Attard, J. R. Owen, *Chem. Mater.*, 14 (2002) 524
26. Y. Tan, S. Srinivasan, K. S. Choi, *J. Am. Chem. Soc.*, 127 (2005) 3596
27. V. Gupta, T. Kusahara, H. Toyama, S. Gupta, N. Miura, *Electrochemistry Communications.*, 9 (2007) 2315
28. D. A. Corrigan, R. M. Bendert, *J. Electrochem. Soc.*, 136 (1989) 723
29. P. V. Kamath, G. N. Subbanna, *J. Appl. Electrochem.*, 22 (1992) 478
30. G. J. D. A. Soler-Illia, M. Jobbagy, A. E. Regazzoni, M. A. Blesa, *Chem. Mater.*, 11 (1999) 3140
31. X. M. Ni, Q. B. Zhao, B. B. Li, J. Cheng, H. G. Zheng, *Solid State Commun.*, 137 (2006) 585
32. P. V. Kamath, M. Dixit, L. Indira, A. K. Shukla, V. G. Kumar, N. Munichandraiah, *J. Electrochem. Soc.*, 141 (1994) 2956
33. J. Jiang, A. Kucernak, *Chem. Mater.*, 16 (2004) 1362
34. J. Jiang, A. Kucernak, *Electrochim. Acta.*, 47 (2002) 2381